SAND2012-0834C

850-nm VCSELs optimized for cryogenic data transmission

Darwin K. Serkland*, Kent M. Geib, Gregory M. Peake, Gordon A. Keeler, Alan Y. Hsu†
Sandia National Laboratories, Albuquerque, NM 87185

ABSTRACT

We report on the development of 850-nm high-speed VCSELs optimized for low-power data transmission at cryogenic temperatures near 100 K. These VCSELs operate on the n=1 quantum well transition at cryogenic temperatures (near 100 K) and on the n=2 transition at room temperature (near 300 K) such that cryogenic cooling is not required for initial testing of the optical interconnects at room temperature. Relative to previous work at 950 nm, the shorter 850-nm wavelength of these VCSELs makes them compatible with high-speed receivers that employ GaAs photodiodes.

Keywords: VCSEL, vertical-cavity surface-emitting laser, optical interconnects, cryogenic sensors, optical transmitters

1. INTRODUCTION

Low-power optical transmitters are being considered for cryogenic sensors and systems that need to transmit high bandwidth data from a cryogenic system (operating at temperatures near 100 K) to a data processor (or memory) operating near room temperature (300 K), as shown schematically in Figure 1. The requirements for such an optical transmitter are: (1) low power dissipation to minimize heating of the cryogenic system, (2) high data bandwidth according to the needs of the particular application, and (3) operation at both cryogenic temperatures (near 100 K) and room temperature (near 300 K), such that the optical interconnect can be tested at room temperature, without the need for cryogenic cooling inside a vacuum cryostat. Vertical-cavity surface-emitting lasers are a natural choice for cryogenic transmitter lasers since they can readily meet the first two requirements, and can be specially designed to operate at widely spaced temperatures. Conventional VCSELs achieve optimum performance over a limited temperature range from 270 to 370 K by aligning the n=1 quantum well gain wavelength with the cavity resonance near 330 K. Previous work produced 950-nm VCSELs that operated with low threshold currents over a wide range of temperatures from 77 K to 370 K by aligning the n=1 and n=2 gain wavelengths with the cavity resonance at the low and high ends of the temperature range, respectively.[1] In this paper, we report on the development of 850-nm VCSELs that utilized strained InGaAs quantum wells to achieve high bandwidth at low bias current and were compatible with standard data communication receivers employing GaAs photodiodes operating at room temperature. Similar to the 950-nm cryogenic VCSELs, gain from the n=2 transition lowered the threshold current at room temperature. Moreover, we have demonstrated high data bandwidth with low power dissipation by measuring eye diagrams at 10 Gb/s over a wide range of operating temperatures from 100 to 300 K.

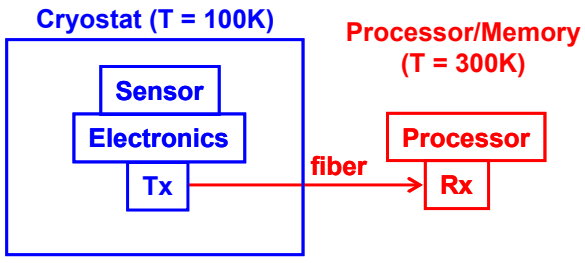

Figure 1. Schematic diagram of a low-power optical data transmitter (Tx) from a cryogenic sensor (or system) to a receiver (Rx) and data processor (or memory) operated near room temperature.

* DKSERKL@sandia.gov; phone: (505) 844-5355; fax: (505) 844-8985; http://www.sandia.gov/
† Current address: Alan Y. Hsu, MIT Lincoln Laboratory, 244 Wood Street, Lexington, MA 02421

2. CRYOGENIC VCSEL DESIGN

In order to achieve a high modulation bandwidth at a low bias current, we chose to employ strained InGaAs quantum wells on a GaAs substrate.[2] As shown schematically in Figure 2(a), the quantum wells were designed to yield useful gain at both the n=1 and n=2 transitions between the conduction band and the heavy hole valence band levels. The n=1 gain wavelength was designed to be 50 nm longer than the VCSEL cavity resonance at T = 300 K, such that when the VCSEL was cooled to 100 K the n=1 gain peak shifted into alignment with the 850-nm cavity resonance wavelength, as shown in Figure 2(b). Hence, the VCSEL was designed to achieve optimum performance at cryogenic temperatures near 100 K. At room temperature (300 K), the n=2 transition provided gain near the 860-nm cavity resonance which helped keep the VCSEL threshold current below 2 mA. The plots in Figure 2(b) show the n=1 and n=2 gain wavelengths and the VCSEL cavity resonance versus temperature, from 100 to 400 K, assuming that the gain tunes at 0.3 nm/K, the cavity tunes at 0.06 nm/K, and the quantum wells were designed to yield a 60 nm splitting between the n=1 and n=2 transitions.

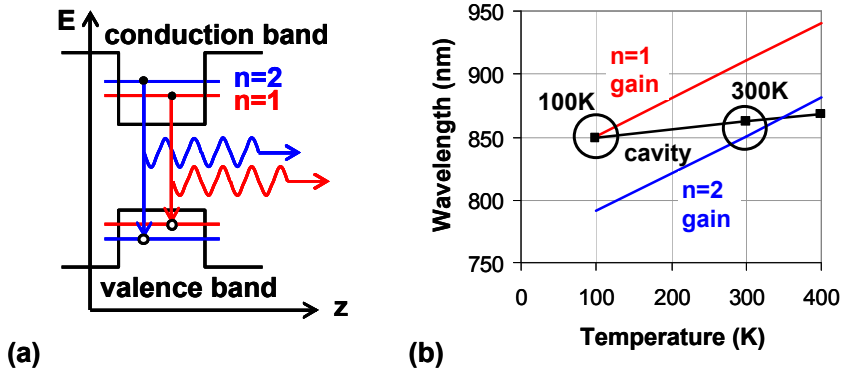

Figure 2. (a) Quantum well design with gain at two wavelengths: n=1 and n=2 transitions from the conduction band to the heavy-hole valence band levels. (b) Plot of gain wavelengths (n=1 and n=2) and cavity resonance wavelength versus temperature.

In contrast to recent high-speed VCSEL designs that employed thin InGaAs quantum wells and high barriers to achieve room-temperature gain at 850 nm, our design utilized thicker quantum wells since cooling from 300 to 100 K shifted the gain wavelength from 910 to 850 nm. Figure 3(a) shows the calculated n=1 and n=2 gain wavelengths at room temperature (300K) for three quantum well width values: 8, 10, and 12 nm. The $In_xGa_{1-x}As$ quantum well was chosen to have an indium composition of $x_W = 0.10$, and the $Al_xGa_{1-x}As$ barrier was chosen to have an aluminum composition of $x_B = 0.10$. Figure 3(b) plots the n=1 and n=2 gain wavelengths versus quantum well width, which clearly shows that the splitting between the two gain peaks narrows as the quantum well width increases.

Quantum Well Designs

Well Indium	Well Width	Barrier Aluminum	C-HH n=1	C-HH n=2
%	nm	%	nm	nm
10	8	10	908	836
10	10	10	916	856
10	12	10	921	872

(a)

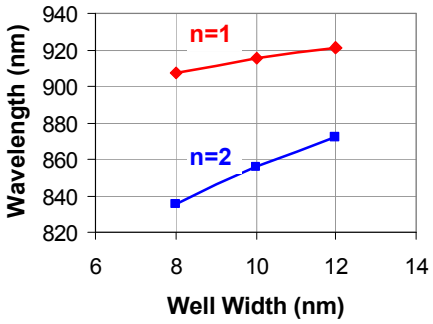

(b)

Figure 3. (a) InGaAs quantum well designs, showing conduction band to heavy hole transition wavelengths for n=1 and n=2. (b) Plot of n=1 and n=2 transition wavelengths at T = 300K versus quantum well width.

The quantum well energy levels were calculated using standard techniques to determine the band gap energies and effective masses of the strained InGaAs quantum wells and un-strained AlGaAs barriers.[3,4] We further assumed that the conduction band offset was 60% of the bandgap difference.

In general, the quantum well width should be chosen based on the temperature separation between the two desired operating temperatures. The results presented in this paper were achieved with a quantum well width of 8 nm, which yielded a wavelength separation of about 70 nm between the n=1 and n=2 gain wavelengths. Figure 4(a) shows the measured photoluminescence (PL) spectrum from a diagnostic wafer containing the same 3-quantum-well active region as the VCSEL wafer, but without the distributed Bragg reflectors (DBRs) and without doping. The n=1 and n=2 transitions from the conduction band to the heavy hole valence band levels appear in Figure 4(a) at the same wavelengths that were predicted in Figure 3(a). The n=2 PL peak appears relatively weak because of the low carrier density that was created by the 1-mW 675-nm pump laser that was focused to a spot diameter of 0.1 mm on the PL wafer. The PL peak near 888 nm is due to the n=1 C-LH (conduction to light hole) transition. Figure 4(b) plots the reflection spectrum of the VCSEL wafer, which shows a cavity resonance near 860 nm at room temperature. As designed, the n=1 gain wavelength was positioned 50 nm longer than the VCSEL cavity resonance at room temperature, such that when the VCSEL was cooled to T = 100 K the n=1 gain shifted into alignment with the 850-nm cavity resonance, yielding a minimum threshold current at cryogenic temperatures.

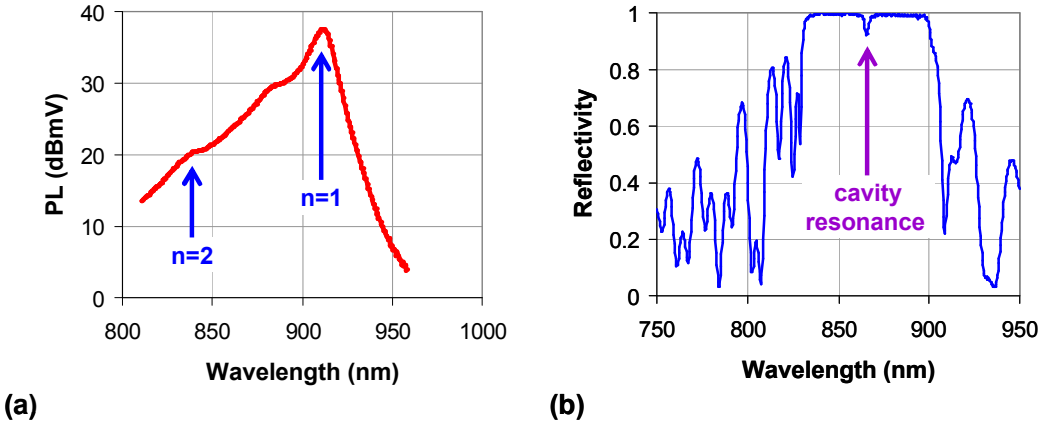

Figure 4. (a) Photoluminescence spectrum at T=300K, showing both n=1 and n=2 conduction to heavy hole transitions. The n=2 emission is relatively weak because of the low carrier density produced by the low-power 675-nm pump laser. (b) Reflection spectrum of the VCSEL wafer at T=300K, showing the DBR stop band and the cavity resonance.

The VCSEL active region employed 3 $In_{0.10}Ga_{0.90}As$ quantum wells, each 8-nm thick as described above, in the middle of a 1-wavelength cavity. Each DBR period contained a high-index $Al_{0.16}Ga_{0.84}As$ layer and a low-index $Al_{0.92}Ga_{0.08}As$ layer, with bi-parabolic grades between them. The top DBR was doped p-type and contained 23 periods, and the bottom DBR was doped n-type and contained 40 periods. The p-type DBR period immediately above the active cavity region contained a quarter-wavelength-thick $Al_{0.98}Ga_{0.02}As$ layer that was selectively oxidized to form a current and optical aperture of diameter 5.5 µm.

3. VCSEL PERFORMANCE VERSUS TEMPERATURE

In this section we discuss the measured performance versus temperature of the cryogenic VCSELs described above. Figure 5(a) shows a cryogenic VCSEL being tested on a probe station at T = 300 K after completion of the micro-fabrication process. The VCSEL mesa diameter of 33.5 µm was oxidized to yield a current and optical aperture of diameter 5.5 µm. After micro-fabrication, the VCSEL chip was mounted on a TO-46 header, top-side wire bonded, and inserted into a vacuum cryostat capable of cooling down to 20K, as shown in Figure 5(b).

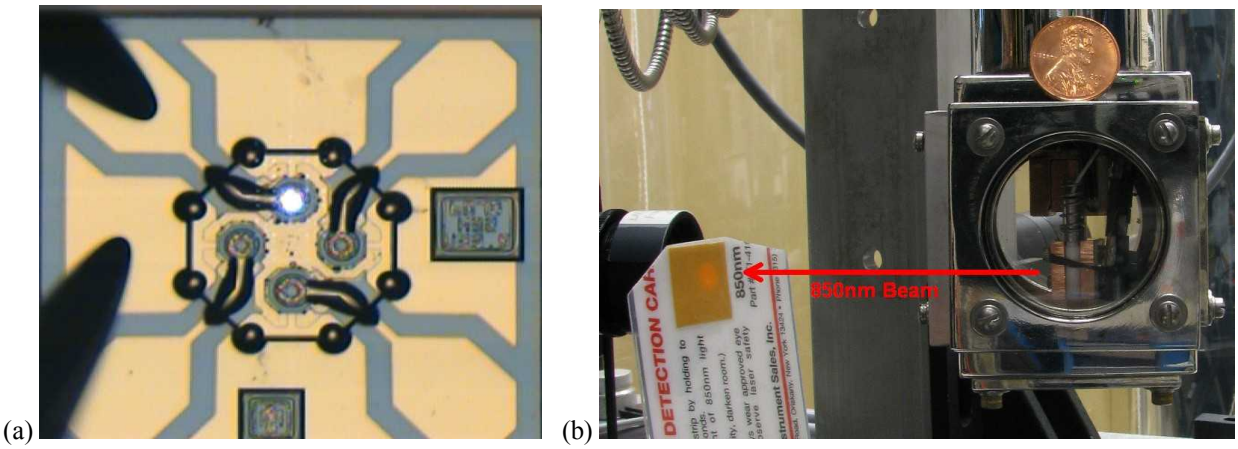

Figure 5. (a) Photograph of the fabricated VCSEL, driven with 3mA current at T=300K. (b) Photograph of the collimated VCSEL output beam striking an infrared detection card, after packaging the VCSEL on a TO-46 header and mounting it in a vacuum cryostat.

Room temperature test results from the VCSEL appear in Figure 6. Figure 6(a) shows the VCSEL optical power and voltage drop versus drive current at T = 300 K. The VCSEL achieved threshold at 1 mA and 1.55 V. The slope efficiency was 0.48 W/A and the series resistance was 79 Ohms. Above threshold the lasing spectrum transitioned from single-moded at 1 mA to dual-moded at 2 mA, with a transverse mode splitting of 0.8 nm, as shown in Figure 6(b).

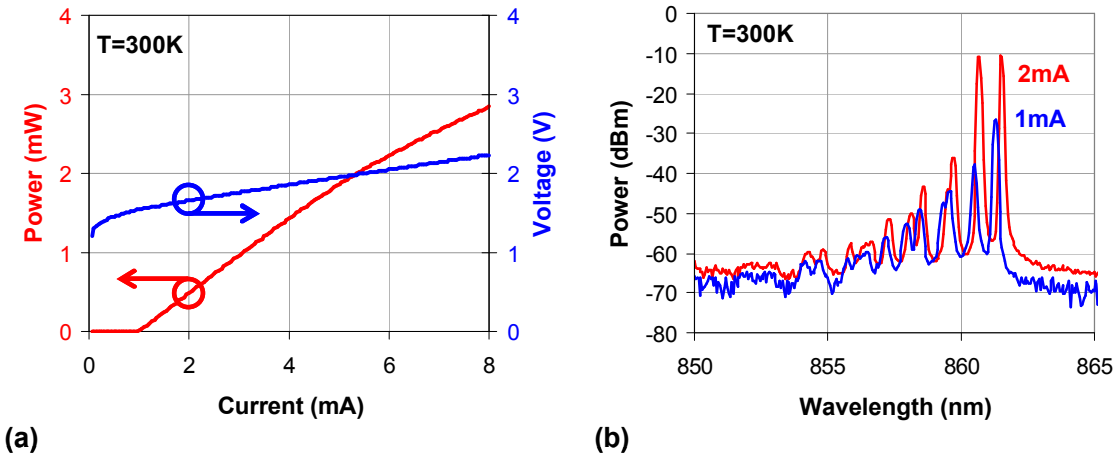

Figure 6. (a) Optical output power and voltage drop versus current at T=300K, showing a threshold current of 1mA. (b) Lasing optical emission spectra at 1 and 2 mA at T=300K.

Figure 7 shows the VCSEL performance, as tested in the vacuum cryostat, over a range of temperatures from 88 to 300 K. As the VCSEL was cooled from 300 K the threshold current decreased and the slope efficiency increased, as the n=1 gain peak shifted into alignment with the 850-nm cavity resonance at approximately T = 120 K. Further cooling below 120 K caused the threshold current to increase rapidly and the slope efficiency to decrease, as the n=1 gain peak shifted to wavelengths shorter than the cavity resonance. As expected, the VCSEL voltage drop at 0.1 mA steadily increased as the device was cooled due to the increase of bandgap energy. The VCSEL series resistance also increased as the device was cooled, due to decreased conductivity of the doped DBRs.

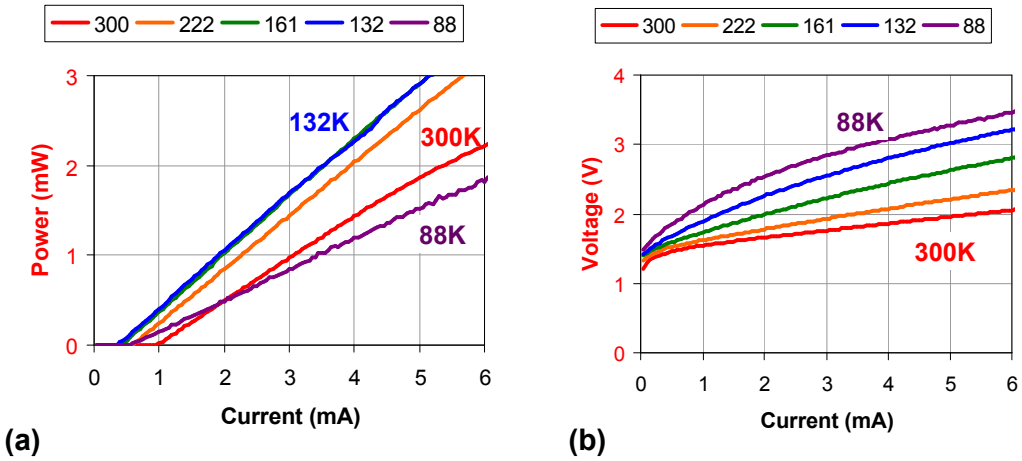

Figure 7. (a) Laser power versus current at temperatures from 88K to 300K. (b) VCSEL voltage versus current at temperatures from 88K to 300K.

Threshold current and differential quantum efficiency (QE) are plotted versus the TO-46 header temperature in Figure 8. Figure 8 clearly shows that the VCSEL achieved minimum threshold current (0.38 mA) and maximum differential quantum efficiency (45%) at a temperature near 120 K, indicating optimum alignment between the n=1 gain wavelength and the cavity resonance at cryogenic temperatures, as intended.

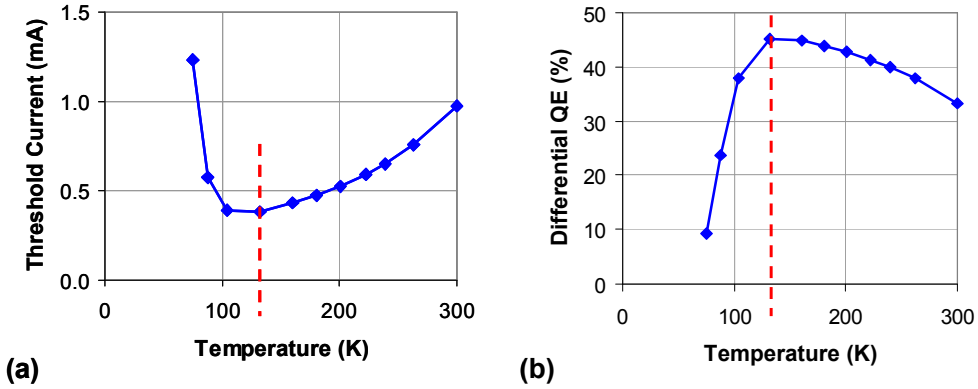

Figure 8. (a) VCSEL threshold current versus temperature, from 88K to 300K. (b) VCSEL differential quantum efficiency versus temperature, from 88K to 300K. Maximum differential quantum efficiency (45%) was achieved at 127K.

The VCSEL emission spectrum at 1 mA is shown in Figure 9(a) at three temperatures from 109 to 301 K. At cryogenic temperatures, near 100 K, the VCSEL emission was single-moded at a 1 mA typical operating current (2.5 times threshold). At room temperature, near 300 K, the VCSEL emission was dual-moded at a 2 mA typical operating current (2 times threshold). Figure 9(b) plots the fundamental transverse mode wavelength versus temperature at 1 mA drive current. The VCSEL cavity resonance tuned at 0.06 nm/K near room temperature and somewhat slower at cryogenic temperatures, as typically observed for 850-nm VCSELs.

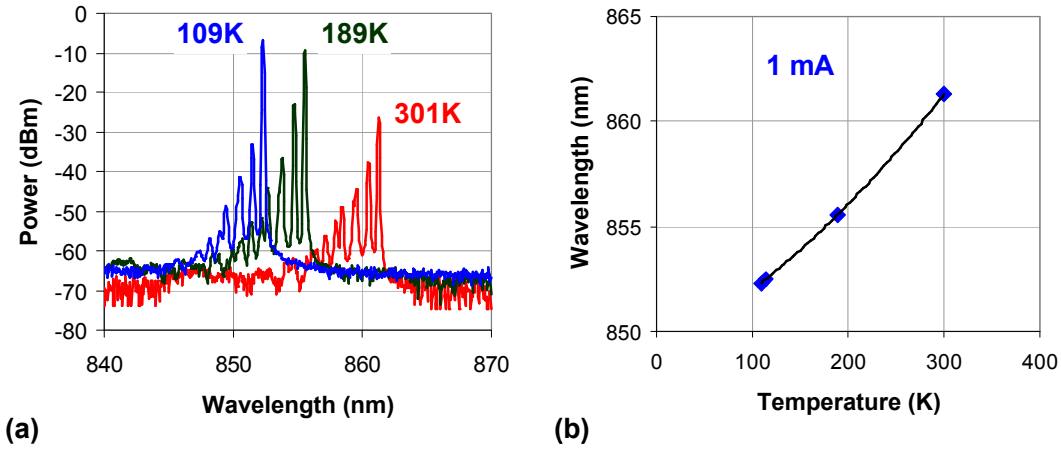

Figure 9. (a) VCSEL emission spectra at 1mA current, measured at 109, 189, and 301K temperatures. (b) Fundamental transverse mode wavelength versus temperature at 1mA drive current, exhibiting an average slope of 0.05 nm/K.

Finally, Figure 10 shows 10 Gb/s eye diagrams obtained at VCSEL temperatures of 300 and 145 K, using a New Focus model 1580-B GaAs photoreceiver with 12 GHz bandwidth. The eye diagram at T = 300 K, shown in Figure 10(a), was obtained at a bias of 2 mA and 1.66 V, yielding an average energy dissipation of 332 fJ/bit. The eye diagram at T = 145 K, shown in Figure 10(b), was obtained at a bias of 1 mA and 1.80 V, yielding an average energy dissipation of 180 fJ/bit. These eye diagrams demonstrate that the cryogenic 850-nm VCSEL achieved the stated goals of low power dissipation and high bandwidth. The eye diagram openings were wider and cleaner at cryogenic temperatures, consistent with the design strategy of optimizing VCSEL performance at cold temperatures. We note that the shape of the eye diagrams changed relatively slowly with temperature, and open eye diagrams were obtained at temperatures slightly below 100 K. However, as the temperature was decreased below 120 K, the increased series resistance and decreased slope efficiency caused the eyes to close in the vertical direction. The vertical eye closing at temperatures below 120 K could be mitigated with increased drive modulation voltage incident on the VCSEL.

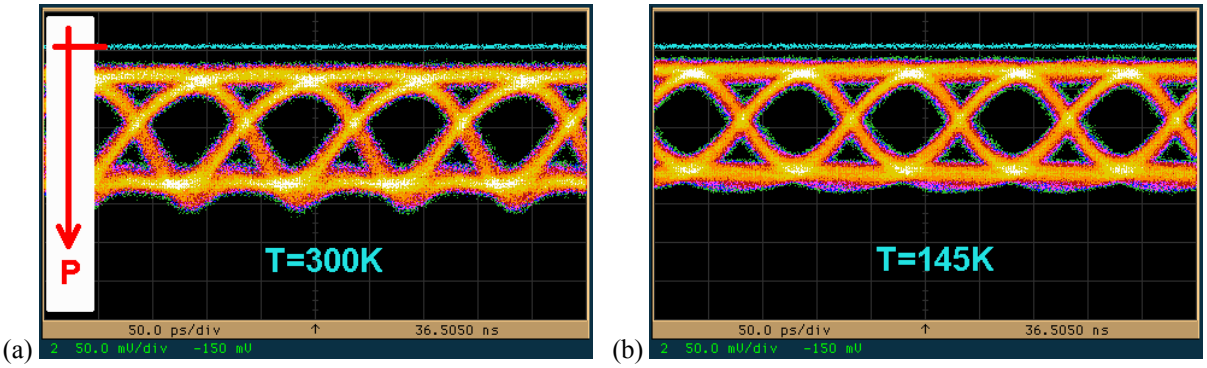

Figure 10. (a) 10Gb/s eye diagram at 300K and 2mA(1.66V) bias. (b) 10Gb/s eye diagram at 145K and 1mA(1.80V) bias.

4. CONCLUSIONS

In conclusion, we have designed, fabricated, and tested 850-nm high-speed VCSELs optimized for low-power data transmission at cryogenic temperatures near 100K. These VCSELs operated on the n=1 quantum well transition at cryogenic temperatures (near 100K) and on the n=2 transition above room temperature (300K) such that cryogenic cooling was not required for initial testing of the optical interconnects at room temperature. Relative to previous work at 950 nm, the shorter 850-nm wavelength of these VCSELs makes them compatible with high-speed receivers that employ GaAs photodiodes.

ACKNOWLEDGMENTS

The authors wish to thank V. M. Sanchez, V. M. Buscema, T. M. Bauer, R. R. Kay and C. T. Sullivan for their expert technical assistance. Sandia National Laboratories is a multi-program laboratory managed and operated by Sandia Corporation, a wholly owned subsidiary of Lockheed Martin Corporation, for the U.S. Department of Energy's National Nuclear Security Administration under contract DE-AC04-94AL85000.

REFERENCES

[1] Y. A. Akulova, B. J. Thibeault, J. Ko, L. A. Coldren, “Low-Temperature Optimized Vertical-Cavity Lasers with Submilliamp Threshold Currents over the 77-370 K Temperature Range,” IEEE Photon. Technol. Lett., vol. 9, pp. 277-279 (1997).

[2] S. B. Healy, E. P. O’Reilly, J. S. Gustavsson, P. Westbergh, A. Haglund, A. Larsson, and A. Joel, “Active Region Design for High-Speed 850-nm VCSELs”, IEEE J. Quantum Electronics, vol. 46, pp. 506-512 (2010).

[3] G. Ji, D. Huang, U. K. Reddy, T. S. Henderson, R. Houdre, and H. Morkoc, “Optical investigation of highly strained InGaAsGaAs multiple quantum wells,” J. Appl. Phys., vol. 62, pp. 3366-3373 (1987).

[4] S. W. Corzine, R. H. Yan, and L. A. Coldren, “Theoretical gain in strained InGaAs/AlGaAs quantum wells including valence band mixing effects,” Appl. Phys. Lett., vol. 57, pp. 2835-2837 (1990).